



Article

# Synthesis, Characterization and Antibacterial Activity of CuS/ZrS<sub>2</sub> Composites Prepared by Precipitation Method

Raghad K. Oudah<sup>1</sup>, Saad S. Mohammed<sup>2</sup>

<sup>1,2</sup> Department of Chemistry, College of Science, University of Thi-Qar, Thi-Qar, 64001, Iraq

\* Correspondence: [raghad.ouda@utq.edu.iq](mailto:raghad.ouda@utq.edu.iq)

**Abstract:** The aim of this research is to investigate the antibacterial activity of CuS/ZrS<sub>2</sub> composites synthesized via the precipitation method. The synthesis involved the combination of zirconium oxychloride octahydrate (ZrOCl<sub>2</sub>·8H<sub>2</sub>O), copper chloride dihydrate (CuCl<sub>2</sub>·2H<sub>2</sub>O), and sodium sulfide (Na<sub>2</sub>S) with ultrasonic irradiation applied at different times (60 and 120 minutes). The resulting nanocomposites were characterized using Field Emission Scanning Electron Microscopy (FESEM), X-ray diffraction (XRD), Energy Dispersive X-ray Spectroscopy (EDS), and UV-VIS-diffuse reflectance spectroscopy. The FESEM analysis revealed the morphology and size of the nanocomposites, with average particle sizes of 40.94 nm and 26.76 nm for CuS/ZrS<sub>2</sub>-60 and CuS/ZrS<sub>2</sub>-120 composites, respectively. XRD analysis confirmed the crystalline structure of the composites. The antibacterial activity of the CuS/ZrS<sub>2</sub> nanocomposites was tested against Gram-negative bacteria (*Escherichia coli* and *Pseudomonas aeruginosa*) and Gram-positive bacteria (*Staphylococcus aureus* and *Enterococcus faecalis*). The composites demonstrated significant antibacterial activity, particularly against *P. aeruginosa* and *E. faecalis*, suggesting their potential for medical and industrial applications.

**Keywords:** Composite, Antibacterial, Nanotechnology, SEM

## 1. Introduction

Nanotechnology refers to everything from the synthesis, processing, characterization and application of materials, devices, and systems through the control of matter on an atomic, molecular, macromolecular and supramolecular scale in a way that exploits novel and enhanced properties and functions, unattainable by the individual constituent materials. In nanosized materials, the size of the constituents or objects primarily controls their physical, chemical, biological, and other properties and functions. Nanomaterials are comprised of materials with grain sizes smaller than 100 nm [1]. Materials with grain sizes as small as 500 nm are known as ultrafine-grained (UFG) materials. A nanocomposite is a multiphase material in which at least one constituent phase has dimensionality in the nanometre-length scale – which is typically smaller than 100 nm.

Composite nanoparticles are produced by combining two different components at the nanoscale, which leads to different behaviours at the physical and chemical level. In this way, the properties of the materials can be combined and new effects occur, taking

**Citation:** Raghad K. Oudah. Synthesis, Characterization and Antibacterial Activity of CuS/ZrS<sub>2</sub> Composites Prepared by Precipitation Method. Central Asian Journal of Medical and Natural Science 2024, 5(4), 291-303.

Received: 10<sup>th</sup> Jul 2024

Revised: 11<sup>th</sup> Agt 2024

Accepted: 24<sup>th</sup> Sep 2024

Published: 27<sup>th</sup> Oct 2024



**Copyright:** © 2024 by the authors. Submitted for open access publication under the terms and conditions of the Creative Commons Attribution (CC BY) license

(<https://creativecommons.org/licenses/by/4.0/>)

advantage of the synergy between them to minimise drawbacks and limitations. Composite nanoparticles present great potentials for application in the manufacturing of new functional materials, energy conversion and storage, wastewater purification, new applications in medical diagnostics and imaging, medical therapies, high performance materials, drug delivery, food packaging, bio-sensors, and electronics and energy industries [2]. Nanocomposites offer new opportunities for the treatment of medical and pharmaceutical products, food packaging, gas and oil machinery, biomedical equipment and implants, and 3D devices. Nanocomposite materials are seen as promising alternatives to microcomposites and monolithic materials, which are the old and unexploited materials of the last century, as they offer new probabilities for applications in partially or fully ceramic, polymer, and metallic materials and the interfacial, multilayer, and hybrid composite structures [3].

Nanocomposites present unique combinations of properties not found in conventional composites from structural constituents whose properties are not novel or special by themselves. Nanocomposites are seen as the materials of the 21st century due to their unique combinations of property due to different design aspects [4]. One of the biggest technologies in materials development is the capability to create in nano meticulousness having the atomic make-up of materials. This paper focuses on the research work on the synthesis and uses of nanomaterials, which has experienced an exponential growth in the last few years [5]. One of the most intriguing observations was that nanocrystals prepared using the modified "nano" approach exhibited a higher surface chemical reactivity than those prepared by using more conventional methods [6]. "Nanocrystalline" semiconductors, such as metal-sulfides, have attracted attention as thermal insulating materials for use in glass. They can show suitable physical and chemical properties such as extremely small size and large surface [7].

More recently, different attempts have been made to regulate the morphology and related spatial organization of metal chalcogenide semiconductor particles [8]. Transition-metal sulfides have wide utility in catalytic and electronic applications because of their high sulfur bond energies, their oxophilicity, as well as their intrinsic electronic and structural [9]. Two-dimensional. Currently, two-dimensional materials have great research potential in the direction of electronic components due to their inherent lightweight (low-dimensional) and high performance (quantitative) [10]. And some of them are used for the fabrication of devices. Their complex structures and valence states result in their interesting physical properties. CuS, known as covellite attracts special interest because it shows a metal-like electrical conductivity down to the liquid-helium temperature [11]. Layered transition metal dichalcogenides  $\text{MX}_2$  ( $\text{M}=\text{Ti, Zr, Hf, Mo, W, V, Nb, and Ta}$ ;  $\text{X}=\text{S and Se}$ ) have unique electronic features due to their large band-edge excitation of the "D-d transition" centered at a metal site. So, these properties lead to a wide range of applications in catalysis and field emission [12].  $\text{ZrS}_2$  material is one of the transition metal chalcogenides and which having several effective responsibilities like environmentally friendly, low-cost availability, highly sensitive, low bandgap energy, and thermodynamic stability [13]. zirconium disulfide ( $\text{ZrS}_2$ ), which has a 1T structure and an appropriate bandgap as a semiconductor, has attracted particular interest. At the atomically thin scale [14]. It has, therefore, become evident that ultrasound is very useful for the synthesis and production of nanoparticles. When liquids are exposed to ultrasound, there is what is known as ultrasonic cavitation.

The cavitation is creating physical and chemical effects like high temperatures and pressures, fast cooling rates, which forms a special environment for the chemical reactions at extreme conditions. To sum up, the preparation of nanoparticles with controllable morphologies by means of ultrasound is an effective method. Its benefits include the synthesis of nanoparticles under room temperature, high rate of the reaction under the use of ultra-sound and thus requires less time for preparation of nanoparticles. This method is relatively fast and simple[15]. It is well known that N and S atoms play a key role in the coordination of metals at the active sites of numerous metallobiomolecules[16]. An antimicrobial agent is one that has the ability to fight viruses, bacteria and or funguses. Antiviral and anti-fungal drugs are compounds which are capable of either killing viruses or preventing their replication, or killing fungi. Antibacterials may be bacteriostatic or bactericidal: bacteriostat prevents the growth of various bacteria, on the other hand bactericide, specialized to kill bacteria[17]. Antibacterial agents are widely used in water treatment and purification, fabrics, food containers, construction materials, pharmaceuticals, and others [18].

Therefore, MDR bacteria are observed in frequent human pathogens such as in *Staphylococcus aureus*, *Enterococcus faecium* and *P. aeruginosa*. Pandrug resistance has been already observed for most of those bacterial species. They may become an unmet medical needs in antibacterial therapy in a near future, occurring to a large extent, mostly but not only in hospital settings [19]. *P. aeruginosa* and *E. faecalis* are two significant pathogens that result in chronic biofilm related infections, more so in the formation of dual species biofilms [20]. Also, bacteria *E. coli* cause some diseases in children, including intestinal infections, diarrhea and bacteria *Staphylococcus aureus*[21]. *Pseudomonas aeruginosa* is a pathogenic bacteria that has the ability to produce an unlimited number of dangerous substances that cause significant tissue damage and delay wound healing [22]. *Enterococcus faecalis* and *Pseudomonas aeruginosa* are important opportunistic human pathogens that cause major problems in medical and food sectors. In fact, *E. faecalis* is a Gram-positive commensal bacterium that is normally associated with human as a member of the gut microflora. However, *E. faecalis* is an opportunistic pathogen of considerable clinical importance, particularly as an etiologic agent of healthcare-associated infections [23]. The aim of this research was to study the antibacterial activity using different types of gram-positive (*E. coli*, *Enterococcus faecalis*) and gram-negative (*Staphylococcus aureus*, *Pseudomonas aeruginosa*) bacterial isolates using CuS/ZrS<sub>2</sub> composites.

## 2. Materials and Methods

### Materials

Copper chloride dihydrate (CuCl<sub>2</sub> · 2H<sub>2</sub>O) %98, Sodium sulfide (Na<sub>2</sub>S) 58-62% from Loba chemie (India). Zirconium oxy chloride octahydrate (ZrOCl<sub>2</sub> · 8H<sub>2</sub>O) %99.5 were purchased from Merck Company (Germany). Sodium hydroxide (NaOH) from Sigma-Aldrich, Hydrochloric acid (BDH) %37. The materials used were of analytical grade and high-purity deionized water was used to dissolve all compounds.

### Methods

Preparation CuS/ZrS<sub>2</sub> composite

Zirconium solution prepared by dissolving (1 gm, 3.10 mmol) of Zirconium oxy Chloride octa hydrate (ZrOCl<sub>2</sub> · 8H<sub>2</sub>O) in 30 ml of de-ionized water with magnetically

stirred. Copper solution prepared by dissolving (0.5 gm, 2.93 mmol) of Copper Chloride dihydrate ( $\text{CuCl}_2 \cdot 2\text{H}_2\text{O}$ ) in 30 ml of de-ionized water. Sodium Sulfide solution prepared by dissolving (1.00 gm, 12.81 mmol) of Sodium Sulfide ( $\text{Na}_2\text{S}$ ) in 30 ml of de-ionized water. CuS/ZrS<sub>2</sub> composite prepared by addition the zirconium solution to Copper solution and heat the solution to a gentle boil on a hot plate, maintaining a temperature of 50-60 °C. Ensure good ventilation as some fumes may be produced and continue stirring for (30 minutes). Then, add sodium sulfide solution slowly (drop by drop) to both the zirconium and copper solution while stirring continuously. Firstly, white precipitate of ZrS<sub>2</sub> formed, and as the addition continues, black precipitate of CuS begins to form. This will cause precipitation of ZrS<sub>2</sub> and CuS. The pH of reaction solution adjusted by addition drops of  $\text{NH}_4\text{OH}$  solution until the pH reaches 9.0. Stir the solution for (30 minutes) to facilitate the complete precipitation of the Sulfides. After the stirring process is completed, the resulted solution is transferred to an ultrasonic device at temperature (30 °C) at different times (60 min, 120 min). After the sonication process completed, the precipitate separated by filtration and the precipitate washed three times firstly with water then with ethanol and later with hexane to remove any impurities. The obtained precipitates dried in an oven at 100 °C for 2 hours to obtain the ZrS<sub>2</sub> and CuS nanocomposite. According to the sonication time, the obtained composites denoted as CuS/ZrS<sub>2</sub>-60, CuS/ZrS<sub>2</sub>-120 minutes sonication time, respectively.

### 3. Results and Discussion

#### 3.1. Characterization

The characterization pattern and phase of studied samples by XRD diffractometer analytical specifying ( $\text{Cu K}\alpha$ ,  $\lambda = 1.54 \text{ \AA}$ ) was applied to calculate crystal size. Field Emission Scanning Electron Microscopy (FEI- Model: Inspect f 50-Netherlands) was applied to get SEM images of the samples a high-energy beam dish of electrons employing. Energy dispersive X-ray spectrometer EDS (Thermo scientific - Netherlands) was using with SEM to describe the formation of samples the composition. The energy gap energies of the prepared CuS/ZrS<sub>2</sub> were calculated by diffuse reflectance spectra using an UV-VIS spectrophotometer (Avantes DH-S-BAL-2048 UV-Vis) in a wavelength range of 230-1100 nm-Netherlands.

##### 3.1.1. UV-vis-diffuse reflectance spectroscopy (UV-vis-DRS)

With regard to semiconductor materials, the absorption wavelengths of the material are closely linked to its bandgap to identify the range of wavelengths at which absorption takes place [24]. To explore the optical properties of the synthesized composites, DRS-UV-Visible- absorption spectra were measured in the range of 250-800 nm. It can be seen in Figures (2,3) that all CuS/ZrS<sub>2</sub>-60, CuS/ZrS<sub>2</sub>-120 composites respectively, exhibit strong visible light absorption which is possibly advantageous for visible light applications. The optical energy band gap of the synthesized composites was measured using the Tauc relation by applying the formula:

$$\alpha h\nu = A (h\nu - E_g)^{1/n} \quad (1)$$

Where,  $\alpha$ ,  $h$ ,  $\nu$ ,  $A$ ,  $E_g$  are the absorption coefficient, Planck's constant, incident light frequency, proportionality constant, and band gap energy respectively. Moreover,  $n$  is a value that depends on the nature of the transition, which is either 2 for a direct transition or 1/2 for an indirect transition. The obtained band gap energy values of CuS/ZrS<sub>2</sub>-60, CuS/ZrS<sub>2</sub>-120 composite are found to be (1.94 eV), (2.0 eV) respectively figures (2,3)

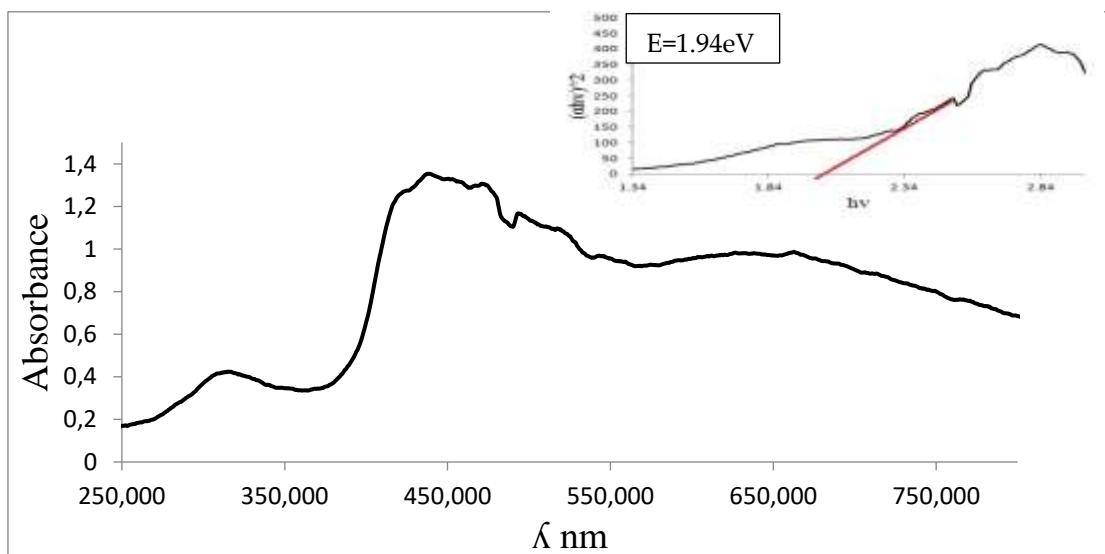


**Figure (2):UV-Visible-DRS absorption spectra and tauc plot of composite CuS/ZrS<sub>2</sub>- 60**

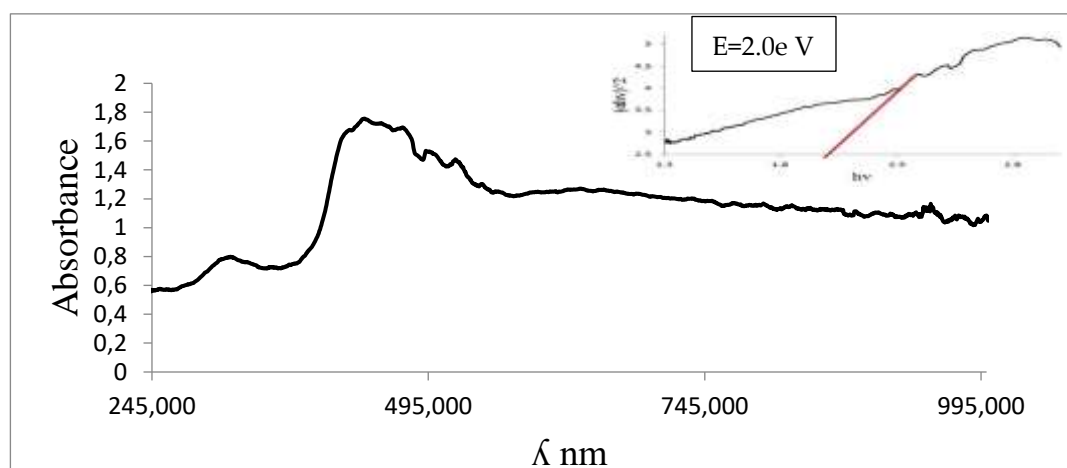


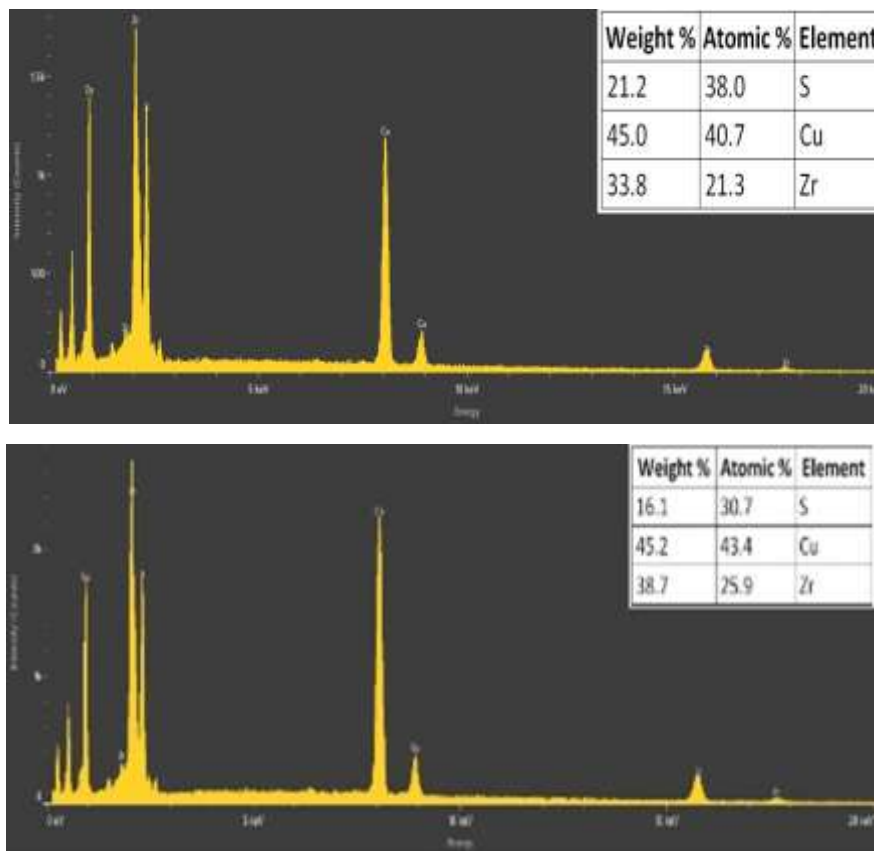
**Figure (3):UV-Visible-DRS absorption spectra and tauc plot of composite CuS/ZrS<sub>2</sub> -120**

### 3.1.2-Energy Dispersive X-ray Spectroscopy(EDS)

According to this reason that when nanoparticles are exposed to them an electron beam then the nanoparticles emit X-rays. Based on this emission the elemental composition of these nanoparticles can be established. An EDS detector that can be placed on a scanning electron microscope counts the number of emitted X-rays to equalize the energy of two electrons. The energy of given off X-ray related to the nature of the element and the given element can be identified qualitatively as well as quantitatively [25]. \

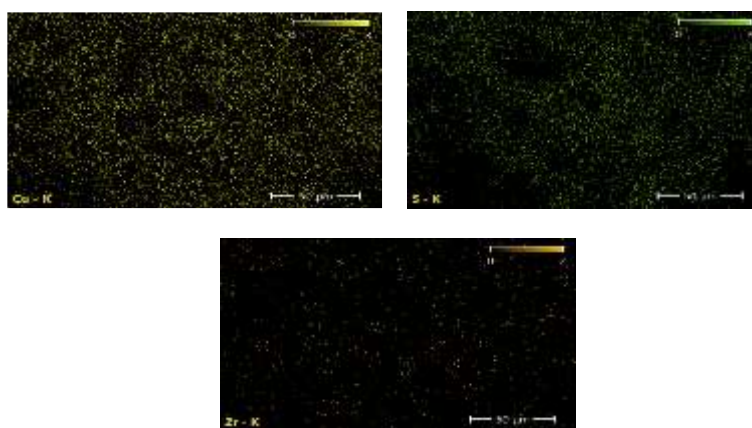
EDS analysis was used to examine the elemental characterization of

CuS/ZrS<sub>2</sub> composites in order to confirm the presence of Cu, Zr, and S in the produced composites. Figures (4,a),(4,b) shows the EDS spectra of CuS /ZrS<sub>2</sub>-60 ,CuS/ZrS<sub>2</sub> -120 ,respectively.

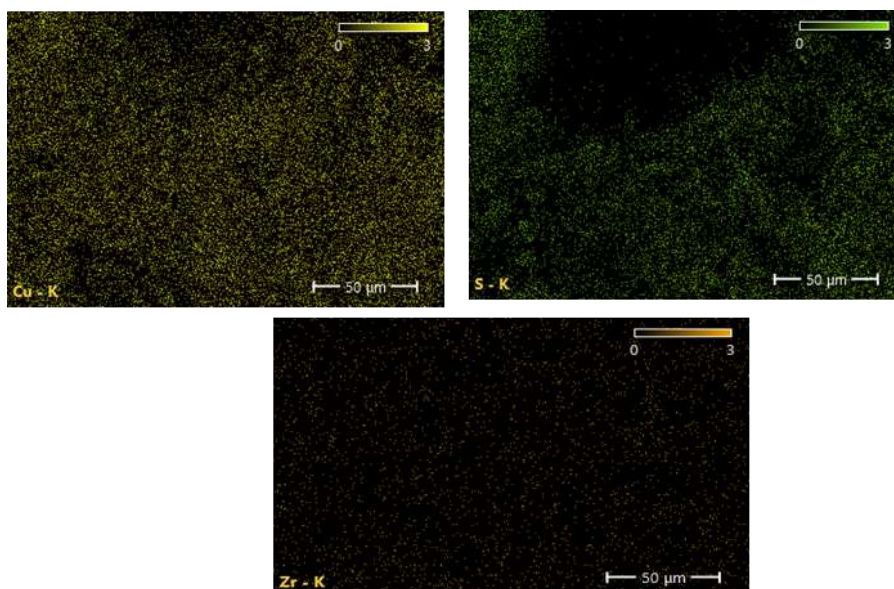


**Figure(4):EDS spectrums of composite (a) CuS/ZrS<sub>2</sub> -60 (b) CuS/ ZrS<sub>2</sub> -120**

EDS results show that all the spectra consisted of Cu, Zr and S peaks without any other contaminants indicating the successful synthesis of pure CuS/ZrS<sub>2</sub> composites. Also, the distribution of Cu, Zr and S throughout the synthesized composites is revealed by the elemental mapping analysis of the composition of the CuS/ZrS<sub>2</sub> composites. Elemental mapping shows the homogenous distribution of Cu, Zr and S across the synthesized composites Figures (5,a),(5,b) for CuS/ZrS<sub>2</sub>-60 ,CuS/ZrS<sub>2</sub>-120,respectively.



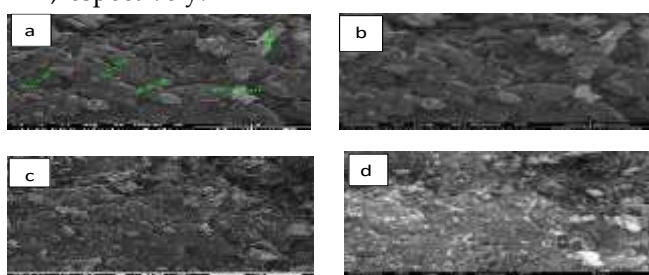
(a)



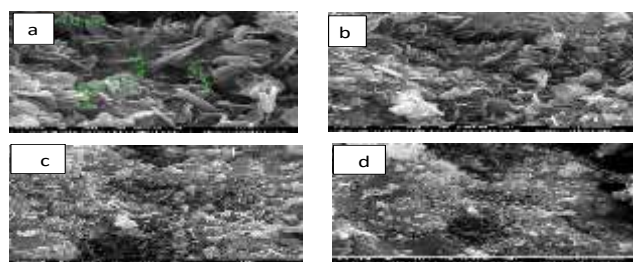
Figure(5):(a) element mapping of CuS/ ZrS<sub>2</sub>- 60 (b)element mapping of CuS/ ZrS<sub>2</sub>-120 composit

### 3.1.3- Field Emission Scanning Electron Microscopy (FESEM):

The morphology and microstructure of the as-prepared CuS / ZrS<sub>2</sub> nanocrystals were studied direct visualization. According to its principles in electron microscopy, includes the following advantages for the morphological and size determination of nanomaterials. Conventionally, a sampling of a particular area of a nanomaterial's surface is made, and one acquires two-dimensional maps illustrating spatial contrasts[25]. The surface morphology and structural features of the (CuS/ZrS<sub>2</sub>) composites were studied using scanning electron microscopy (SEM). The sizes of the synthesized composites within the nanometer range, and they had non-homogenous structures as shown in figures (6,7). The shapes of the synthesized composites were plate shaped and rod- plate Shaped for CuS/ZrS<sub>2</sub> -60, CuS/ZrS<sub>2</sub> -120 composites respectively , and the average particle size was calculated 40.94 nm , 26.76 nm ,respectively.



Figure(6): SEM images of composite CuS/ZrS<sub>2</sub>-60 (a)500nm(b) 1μm (c)3μm (d) 5μm



Figure(7): SEM images of composite CuS/ZrS<sub>2</sub>-120 (a)500nm(b) 1μm (c)3μm (d) 5μm

### 3.1.4. X-ray-Based Characterization

X-ray diffraction or also known as XRD is one of the most popular methods that are used in structure characterization of nanomaterials. XRD works under the efficient interference of monochromatic X-rays and Bragg's law. The diffraction of an X-ray beam in scattering from a crystalline surface is defined by the Bragg's law which is the function of the wavelength of the X-ray, scattering angle, and inter-planar distance as stated in Equation (2).

$$n\lambda = 2d \sin\theta \quad (2)$$

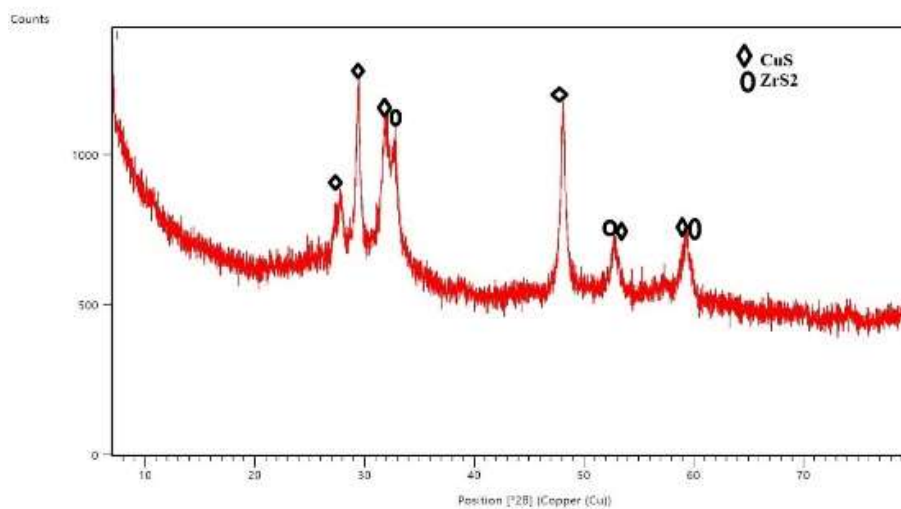
For example in Bragg's law the variable  $d$  symbolizes the inter planar spacing,  $\theta$  is the incidence angle,  $\lambda$  the wavelength of the radiation and  $n$  is the diffraction order. The composition of nanoparticles can be compared with the reference patterns originated from international centre for diffraction data (ICDD).

From a small quantity of powdered sample and the formula (Equation 3) due to Debye – Scherrer, one can also find the lattice parameter of the material as well as the nature of its phase and the size of the crystalline grains. Here,  $(D)$  signifies the crystallite size while  $(k)$  is Scherrer's constant that is equal to 0.94,  $(\beta)$  is F.W.H.M and finally  $(\theta)$  is the position of the said peak [26].

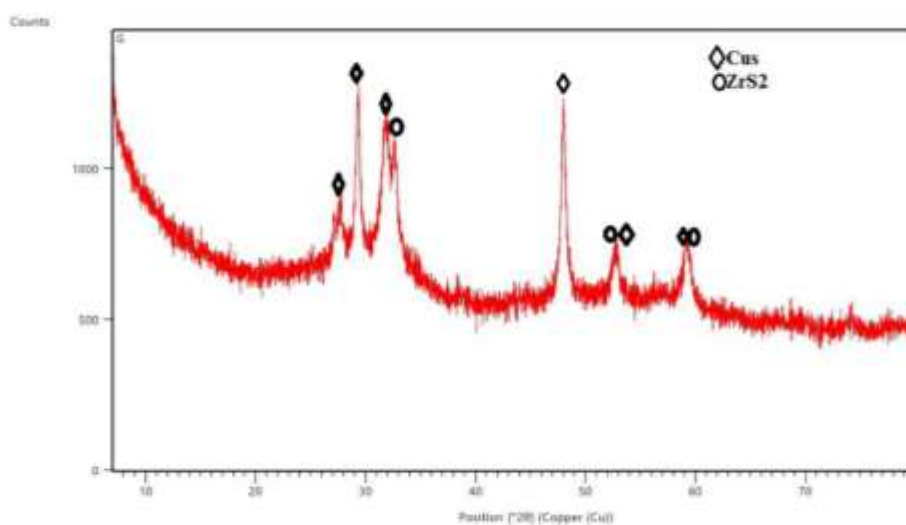
$$D = \frac{k\lambda}{\beta \cos\theta} \quad (3)$$

XRD was used to analyze the crystal structure of the synthesized CuS/ZrS<sub>2</sub> composites and the results showed in figures (CuS/ZrS<sub>2</sub>-60, CuS/ZrS<sub>2</sub>-120). It can be seen that all composites have ZrS<sub>2</sub> and CuS phases, as compared with the zirconium sulfide standard (JCPDS card no. 11-0679)[2] and the Copper sulfide standard (JCPDS card no. 24-0060)[1] respectively. The average crystallite size of the nanoparticles, as estimated using Scherrer equation.

The average crystallite size the average 11.23nm for CuS/ZrS<sub>2</sub>-60, 10.72 nm for CuS/ZrS<sub>2</sub>-120. As seen in figure (8,a), the composite exhibits broad diffraction peaks, and the major diffraction peaks at  $2\theta = 27.57, 29.40, 31.93, 48.07, 52.77, 59.20$  correspond to the (101), (106), (103), (107), (108) and (116) lattice planes respectively, which can be assigned to the CuS phase. ZrS<sub>2</sub> diffraction peak appears at  $2\theta = 32.75$  related to (101) plan and the other diffraction peaks related to ZrS<sub>2</sub> (111) and (201) planes merged with CuS peaks and appears as a single peaks at the same  $2\theta$  range of CuS. As seen in figure(8,b), the composite exhibits broad diffraction peaks, and the major diffraction peaks at  $2\theta = 27.40, 29.29, 31.82, 47.97, 52.7, 59.15$  correspond to the (101), (106), (103), (107), (108) and (116) lattice planes respectively, which can be assigned to the CuS phase. ZrS<sub>2</sub> diffraction peak appears at  $2\theta = 32.65$  related to (101) plan and the other diffraction peaks related to ZrS<sub>2</sub> (111) and (201) planes merged with CuS peaks and appears as a single peaks at the same  $2\theta$  range of CuS.



(a)



(b)

Figure(8):XRD patterns of Composites (a) CuS/ZrS<sub>2</sub> -60 (b) CuS/ZrS<sub>2</sub>-120

#### 4-Antibacterial activity

The antibacterial activity was studied using different types of bacterial isolates : positive bacteria, *Enterococcus faecalis* and negative bacteria, *Pseudomonas aeruginosa* . *Escherichia coli*( ATCC 25922) is a gram-negative bacteria which is a normal inhabitant of the humans as well as animals' intestine while *Staphylococcus aureus* (ATCC 25923) is a gram-positive bacteria which frequently

reside in individuals' respiratory tract and skin. These are the two main bacteria accountable to nosocomial diseases [27].

These types of bacteria were chosen because of their importance in medicine and because they cause some diseases. Plates were chosen for each type and with different concentrations( 40,30,20,10  $\mu\text{g/ml}$ ) of CuS/ZrS<sub>2</sub> dissolved in dimethyl sulfoxide for each type for the purpose of testing the antibacterial effectiveness of the model, the control was dimethyl sulfoxide. The agar well diffusion method was used to detect the activity of the samples each bacterial isolate under study was grown in nutrient broth and incubated at 37 °C for 18-24 hrs [28]. The diameter of the inhibition zone was measured in millimeters using the inhibition zone method after inhibition occurred. Inhibition was measured for the bacterial isolates used after 24 hours, and the results obtained were recorded in the table (1), which represents the negative (*Pseudomonas aeruginosa*, *E. coli*) and positive (*Staphylococcus aureus*, *Enterococcus faecalis*) bacterial isolates with different concentrations of the compound. CuS/ZrS<sub>2</sub> composite .

The effectiveness of the compound was determined by measuring the diameter of the inhibition zone in millimeters using the inhibition zone method where the results showed against positive bacterial isolates. *Enterococcus faecalis* and negative *Pseudomonas aeruginosa* For the compound CuS/ZrS<sub>2</sub> composite, the results showed that the nanocomposite possesses antibacterial activity, which was inferred from measuring the diameter of the inhibition zone, where the diameter of the inhibition zone was equal to 20 mm, 16 mm, for bacteria (*Enterococcus faecalis*), and 22 mm, 18 mm for bacteria (*Pseudomonas aeruginosa*). As for the rest of the bacterial isolates, the compound has no effect as an effective antibiotic.

**Table(1): Biological activity against types of bacterial isolates of the prepared compound**

Type	Zoon of Inhibition (1)	Zoon of Inhibition (2)
<b><i>Pseudomonas aeruginosa</i></b>	22	18
<b><i>Enterococcus faecalis</i></b>	20	16
<b><i>Staphylococcus aureus</i></b>	----	----
<b><i>E. Coli</i></b>	----	----

#### 4. Conclusion

In this work CuS/ZrS<sub>2</sub> nanocomposites were prepared by precipitation and ultrasonic assisted method. In order to examine the shape and size of the as-prepared samples, FESEM analysis was used. The structural information of the produced materials was characterized by X-ray diffraction (XRD) patterns while, the optical performance of the prepared nanostructures was analyzed using ultraviolet-visible (UV-Vis) spectroscopy. The study showed that the average crystallite size of the nanoparticles, as estimated using Scherrer equation are 11.23 nm for ZrS<sub>2</sub>/CuS -60, 10.72 nm for ZrS<sub>2</sub>/CuS-120. The morphology and microstructure of the as-prepared CuS/ZrS<sub>2</sub> nanocrystals were studied with FESEM. The shapes of the synthesized composites were plate shaped and rod-plate shaped for CuS/ZrS<sub>2</sub> -60, CuS/ZrS<sub>2</sub>-120 composites respectively and the average particle size was calculated 40.94 nm, 26.76 nm, respectively. Particle size measured by FESEM larger than crystallite size measured by XRD which refer to the polycrystalline nature of CuS/ZrS<sub>2</sub> nanoparticles. The EDS spectrum confirms the presence of Zirconium (Zr), copper (Cu) and sulphur (S), in all samples. Plotting the Tauc plot and extrapolating the data we found that the band gap is came out to be (1.94 eV, 2.0 eV), respectively in UV-vis-diffuse reflectance spectroscopy. The antibacterial activity was studied using four types of bacteria: positive bacteria (and negative bacteria) with different concentrations of the studied compound. The results were (16, 20 mm) for the positive bacteria (*Enterococcus faecalis*) and (18, 22 mm) for the negative bacteria (*Pseudomonas aeruginosa*). Other bacterial isolates did not show any biological activity with the nanocomposite.

#### REFERENCES

- [1] Palmero, P., "Structural ceramic nanocomposites: a review of properties and powders' synthesis methods," *\*Nanomaterials\**, vol. 5, no. 2, pp. 656-696, 2015.
- [2] Yasin, S. A., et al., "The efficient removal of methylene blue dye using CuO/PET nanocomposite in aqueous solutions," *\*Catalysts\**, vol. 11, no. 2, p. 241, 2021.
- [3] Omanović-Miklićanin, E., et al., "Nanocomposites: A brief review," *\*Health and Technology\**, vol. 10, pp. 51-59, 2020.
- [4] Camargo, P. H. C., K. G. Satyanarayana, and F. Wypych, "Nanocomposites: synthesis, structure, properties and new application opportunities," *\*Materials Research\**, vol. 12, pp. 1-39, 2009.
- [5] Guo, Q.-Z., et al., "Synthesis, characterization and application of magnetic-zirconia nanocomposites," *\*Journal of Non-Crystalline Solids\**, vol. 355, no. 16-17, pp. 922-925, 2009.
- [6] Godočiková, E., et al., "Thermal behaviour of mechanochemically synthesized nanocrystalline CuS," *\*Thermochimica Acta\**, vol. 440, no. 1, pp. 19-22, 2006.
- [7] Jung, D., et al., "The effect of pH on crystal characteristics and IR absorbance of copper sulfide nanoparticles," *\*Journal of Nanoscience and Nanotechnology\**, vol. 13, no. 10, pp. 7169-7172, 2013.
- [8] Zou, J., et al., "Synthesis and characterization of copper sulfide nanocrystal with three-dimensional flower-shape," *\*Journal of Materials Science\**, vol. 42, pp. 9181-9186, 2007.
- [9] Thiyagarajan, R., M. M. Beevi, and M. Anusuya, "Nano structural characteristics of zirconium sulphide thin films," *\*J. Am. Sci.\**, vol. 5, no. 3, p. 26, 2009.

- [10] Song, Q., et al., "Strain-Tuned Structural, Mechanical and Electronic Properties of Two-Dimensional Transition Metal Sulfides ZrS<sub>2</sub>: A First Principles Study," 2021.
- [11] Grijalva, H., et al., "Amorphous and crystalline copper sulfides, CuS," *\*Journal of Materials Chemistry\**, vol. 6, no. 7, pp. 1157-1160, 1996.
- [12] Li, L., et al., "High-performance Schottky solar cells using ZrS<sub>2</sub> nanobelt networks," *\*Energy & Environmental Science\**, vol. 4, no. 7, pp. 2586-2590, 2011.
- [13] Gnanamoorthy, G., et al., "A new CuZr<sub>2</sub>S<sub>4</sub>/rGO and their reduced graphene oxide nanocomposites enhanced photocatalytic and antimicrobial activities," *\*Chemical Physics Letters\**, vol. 781, p. 139011, 2021.
- [14] Otomo, M., et al., "Chemical states of PVD-ZrS<sub>2</sub> film underneath scaled high-k film with self-oxidized ZrO<sub>2</sub> film as interfacial layer," *\*Japanese Journal of Applied Physics\**, vol. 62, no. SC, p. SC1015, 2023.
- [15] Rane, A. V., et al., "Methods for synthesis of nanoparticles and fabrication of nanocomposites," in *\*Synthesis of Inorganic Nanomaterials\**, Elsevier, 2018, pp. 121-139.
- [16] Bagihalli, G. B., et al., "Synthesis, spectral characterization, in vitro antibacterial, antifungal and cytotoxic activities of Co (II), Ni (II) and Cu (II) complexes with 1, 2, 4-triazole Schiff bases," *\*European Journal of Medicinal Chemistry\**, vol. 43, no. 12, pp. 2639-2649, 2008.
- [17] Rameshbabu, N., et al., "Antibacterial nanosized silver substituted hydroxyapatite: synthesis and characterization," *\*Journal of Biomedical Materials Research Part A\**, vol. 80, no. 3, pp. 581-591, 2007.
- [18] Gordon, T., et al., "Synthesis and characterization of zinc/iron oxide composite nanoparticles and their antibacterial properties," *\*Colloids and Surfaces A: Physicochemical and Engineering Aspects\**, vol. 374, no. 1-3, pp. 1-8, 2011.
- [19] Nordmann, P., et al., "Superbugs in the coming new decade; multidrug resistance and prospects for treatment of *Staphylococcus aureus*, *Enterococcus* spp. and *Pseudomonas aeruginosa* in 2010," *\*Current Opinion in Microbiology\**, vol. 10, no. 5, pp. 436-440, 2007.
- [20] Lee, K., et al., "Molecular determinants of the thickened matrix in a dual-species *Pseudomonas aeruginosa* and *Enterococcus faecalis* biofilm," *\*Applied and Environmental Microbiology\**, vol. 83, no. 21, p. e01182-17, 2017.
- [21] Al-Jalili, A. K. J. A.-R. H. I. A. I. J. H., "Extraction of glycomacropptide protein from cheese whey and its use as an antibacterial against *Escherichia coli* and *Staphylococcus aureus* in children," *\*Dhi Qar Science Journal\**, 2013.
- [22] Hussein, K. R., "Molecular feature of *lasB* gene of *Pseudomonas aeruginosa* isolated from different clinical sources," *\*University of Thi-Qar Journal Of Science\**, 2018.
- [23] Mechmechani, S., et al., "Microencapsulation of carvacrol as an efficient tool to fight *Pseudomonas aeruginosa* and *Enterococcus faecalis* biofilms," *\*PLoS One\**, vol. 17, no. 7, p. e0270200, 2022.
- [24] An, H., et al., "Synthesis and characterization of TiO<sub>2</sub>/CuS nanocomposite fibers as a visible light-driven photocatalyst," *\*Journal of the Korean Ceramic Society\**, vol. 55, no. 3, pp. 267-274, 2018.
- [25] Patra, J. K., and K.-H. Baek, "Green nanobiotechnology: factors affecting synthesis and characterization techniques," *\*Journal of Nanomaterials\**, vol. 2014, p. 219, 2015.
- [26] Paras, et al., "A review on low-dimensional nanomaterials: nanofabrication, characterization and applications," *\*Nanomaterials\**, vol. 13, no. 1, p. 160, 2022.

- [27] Guisbiers, G., et al., "Inhibition of E. coli and S. aureus with selenium nanoparticles synthesized by pulsed laser ablation in deionized water," *\*International Journal of Nanomedicine\**, p. 3731-3736, 2016.
- [28] Martina, L. P., et al., "An in vitro comparative antibacterial study of different concentrations of green tea extracts and 2% chlorhexidine on Enterococcus faecalis," *\*Saudi Endodontic Journal\**, vol. 3, no. 3, p. 1, 2013.